MINERAL CHEMISTRY AND ^{40}Ar/^{39}Ar DATING OF MUSCOVITE FROM THE EAST KEMPTVILLE LEUCOGRANITE, SOUTHERN NOVA SCOTIA: EVIDENCE FOR LOCALIZED RESETTING OF ^{40}Ar/^{39}Ar SYSTEMATICS IN A SHEAR ZONE

DANIEL J. KONTAK

Nova Scotia Department of Natural Resources, P.O. Box 698, Halifax, Nova Scotia B3J 2T9

EDWARD FARRAR AND SANDRA McBRIDE

Department of Geological Sciences, Queen's University, Kingston, Ontario K7L 3N6

ROBERT F. MARTIN

Department of Earth and Planetary Sciences, McGill University, Montreal, Quebec H3A 2A7

ABSTRACT

The East Kemptville topaz–muscovite leucogranite, part of the 370 Ma peraluminous South Mountain Batholith of southern Nova Scotia, experienced a complex thermal evolution. A variety of geochronological studies (Pb–Pb, U–Pb, Rb/Sr, ^{40}Ar/^{39}Ar) indicate that after initial emplacement at *ca.* 370 Ma, variable resetting of radiometric systems occurred until *ca.* 240 Ma. The presence of mylonitic zones, *C–S* fabrics and spaced cleavage within the leucogranite indicate that it is located within a high-strain zone, the East Kemptville – East Dalhousie Fault, one of several regionally extensive fault zones transecting the South Mountain Batholith. The present study combines results of electron-microprobe analyses, X-ray diffraction and ^{40}Ar/^{39}Ar step-heating experiments on seven grain-size fractions (550 to 175 µm) of muscovite from a sample of leucogranite to determine the influence of chemistry and grain size on argon diffusivity. The similar composition of the size fractions, presence of a single polytype ($2M_1$) and discordant but comparable ^{40}Ar/^{39}Ar age spectra indicate that argon diffusion was not controlled by differences in mineral chemistry, a mixture of polytypes or differences in apparent grain-size. Although a regional thermal overprinting event and mixing of grain-size fractions of different ages are considered as potential explanations for the discordances in the age spectra, the most likely reason is diffusive loss of argon controlled by an effective grain-size smaller than the finest size-fraction prepared (<175 µm); the effective grain-size was controlled by development of microstructures and subtle chemical heterogeneity. Thus, the variably discordant ^{40}Ar/^{39}Ar age spectra of muscovite from this area are considered to reflect structural focusing of heated fluids that was facilitated by the inherent anisotropy of the host leucogranite (*i.e.*, shear zones).

Keywords: ^{40}Ar/^{39}Ar dating, tin mineralization, muscovite, chemical composition, shear zones, leucogranite, East Kemptville, Nova Scotia.

SOMMAIRE

Le leucogranite à topaze et muscovite de East Kemptville, qui fait partie du batholite de South Mountain, au sud de la Nouvelle-Écosse, a subi une évolution thermique complexe. Les résultats d'études géochronologiques (Pb–Pb, U–Pb, Rb/Sr, ^{40}Ar/^{39}Ar) témoignent d'un remaniement variable des systèmes radiométriques après la mise en place il y a environ 370 million d'années, pendant un intervalle jusqu'à environ 240 Ma. La présence de zones mylonitiques, des microtextures *C–S*, et de clivages espacés dans le leucogranite témoignent de l'importance d'une zone de déformation locale relativement intense, la faille de East Kemptville – East Dalhousie, une parmi plusieurs failles régionales recoupant le batholite de South Mountain. Nous présentons les résultats d'une étude de la muscovite par microsonde électronique et par diffraction X, et de sept concentrés classés selon la taille des grains (de 550 à 175 µm), et chauffés par étapes afin d'assurer la libération de ^{40}Ar et de ^{39}Ar. Notre but était de caractériser l'influence qu'ont la composition chimique et la granulométrie sur la diffusivité de l'argon. La composition chimique à peu près constante, la présence d'un seul polytype ($2M_1$), et les spectres ^{40}Ar/^{39}Ar discordants mais tout de même comparables démontrent que la diffusivité de l'argon n'a pas été influencée par les variations chimiques, par la présence d'un mélange de polytypes, ou par des variations dans la granulométrie apparente. Quoiqu'un événement de réchauffement régional et un mélange de granulométries pourraient expliquer les spectres d'âge, nous attribuons la perte de l'argon par diffusion à partir de domaines d'une granulométrie effective inférieure à la taille la plus petite que nous avons isolée (<175 µm). La granulométrie effective a été influencée par le développement de microstructures et d'hétérogénéités subtiles en composition. Les discordances relevées dans les spectres d'âge ^{40}Ar/^{39}Ar de la muscovite de cette région résulteraient de la focalisation d'une phase fluide chauffée, dont la circulation a été facilitée par l'anisotropie du leucogranite hôte, c'est-à-dire, la présence des zones de cisaillement.

(Traduit par la Rédaction)

Mots-clés: datation ^{40}Ar/^{39}Ar, minéralisation en étain, composition chimique, muscovite, zones de cisaillement, leucogranite, East Kemptville, Nouvelle-Écosse.

INTRODUCTION

The application of $^{40}Ar/^{39}Ar$ incremental step-heating studies has successfully resolved the timing of tectonothermal events in orogenic belts (Dallmeyer 1975, Dallmeyer & Keppie 1987, Muecke et al. 1988, Harrison et al. 1989, Wright & Dallmeyer 1991, Haggart et al. 1993), thermal overprinting in contact aureoles (Berger 1975, Hanson et al. 1975, Harrison & McDougall 1980), and deformation in shear zones (Costa & Maluski 1988, Goodwin & Renne 1991, West & Lux 1993). This is possible because of the dependence of Ar diffusivity on physical and chemical parameters [McDougall & Harrison (1988) and references therein]. For example, in a slowly cooled terrane, minerals with high activation energies of Ar diffusivity (e.g., amphibole: Harrison 1980, Baldwin et al. 1990) will give older ages than minerals with lower activation energies [e.g., K-feldspar (Foland 1974) or biotite (Harrison et al. 1985)]. Consequently,

it is possible to determine a cooling curve for a thermally disturbed area by dating several coexisting K-bearing phases (e.g., Berger & York 1981). However, one parameter, grain size, is known to influence the extent of Ar loss by diffusion, but is rarely considered in $^{40}Ar/^{39}Ar$ studies, despite the fact that it has been known to be important since Dodson (1973) formulated equations relating diffusivity and blocking temperatures. A few cases illustrate this point: (1) Berger & York (1981) analyzed two size fractions of biotite from an intrusive rock (Glamorgan complex, Haliburton, Ontario) and obtained apparent plateau ages of 905 Ma (500 μm grains) and 955 Ma (1500 μm grains); (2) in the case of a Pliocene granite from the Caucasus, Russia, Hess et al. (1993) found that a time–temperature path could be determined exclusively by $^{40}Ar/^{39}Ar$ dating of different grain-size fractions of a single mineral (biotite in that case); and (3) Zweng et al. (1993) analyzed different size-fractions of hydrothermal muscovite and biotite in
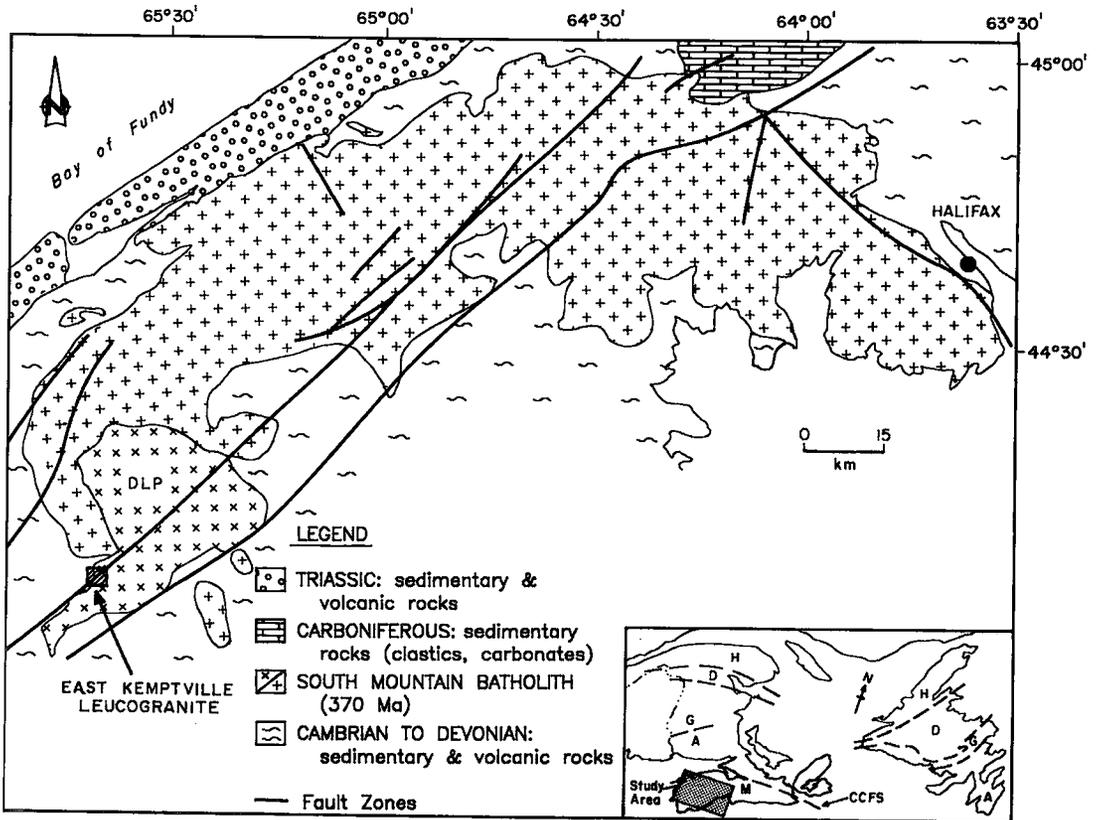

FIG. 1. Simplified geological map of southern Nova Scotia showing the extent of the South Mountain Batholith, outline of the Davis Lake pluton (DLP), location of the East Kemptville leucogranite and tin deposit, and terranes of the Appalachian Orogen in the inset (after Williams & Hatcher 1983). Abbreviations: A, Avalon; M, Meguma; G, Gander; D, Dunnage; H, Humber; CCFS, Cobequid–Chedabucto Fault System.

their thermochronological study of gold-bearing quartz veins of the Camflo deposit, Quebec, and with these data deduced rates of cooling and uplift.

The East Kemptville leucogranite, southwestern Nova Scotia (Figs. 1, 2), forms part of the 370 Ma South Mountain Batholith (MacDonald et al. 1992). The leucogranite is important economically because it hosts a major tin deposit which, until its recent closure (in January, 1992), was the only primary producer of tin in North America. In order to establish the age of the host leucogranite and related mineralization, several geochronological studies (U/Pb, Pb–Pb, Rb/Sr, $^{40}Ar/^{39}Ar$) have been completed (Table 1). Collectively, the age data indicate that the leucogranite experienced a complex thermal history in response to reactivation of a fault zone (East Kemptville – East Dalhousie Fault; EKEDFZ in Fig. 2) within which it resides (Kontak & Cormier 1991). Four previous $^{40}Ar/^{39}Ar$ age spectra for muscovite indicate markedly different profiles, with apparent plateau ages of ca. 295 to 350 Ma, despite the fact that these samples come from a small area (<1 km^2; Fig. 2). To assess the reason for these variably discordant age spectra, $^{40}Ar/^{39}Ar$ step-heating experiments and geochemical analyses of grain-size fractions of muscovite from a single,

relatively undeformed sample of leucogranite were undertaken. These data should permit assessment of the influence of grain size and chemical composition on rate of Ar diffusion, and of the importance of these parameters in affecting the apparent $^{40}Ar/^{39}Ar$ ages observed. In a similar study, West & Lux (1993) focused on a determination of the age of mylonitization within a fault zone in Maine by analyzing different size-fractions of muscovite.

GEOLOGICAL SETTING

The study area is located within the Meguma Terrane of the Canadian Appalachians (Fig. 1). Two lithotectonic units dominate the geology of this terrane, namely metaturbidites of the Cambro-Ordovician Meguma Group and bodies of late Devonian peraluminous granite, such as the South Mountain Batholith. The area was penetratively deformed during the mid-Devonian Acadian Orogeny, which records the docking of the Meguma Terrane with ancestral North America along the Cobequid–Chedabucto Fault System (CCFS in Fig. 1); an age of 400 ± 10 Ma is estimated for this event based on whole-rock $^{40}Ar/^{39}Ar$ dating (Reynolds & Muecke 1978, Muecke et al. 1988,
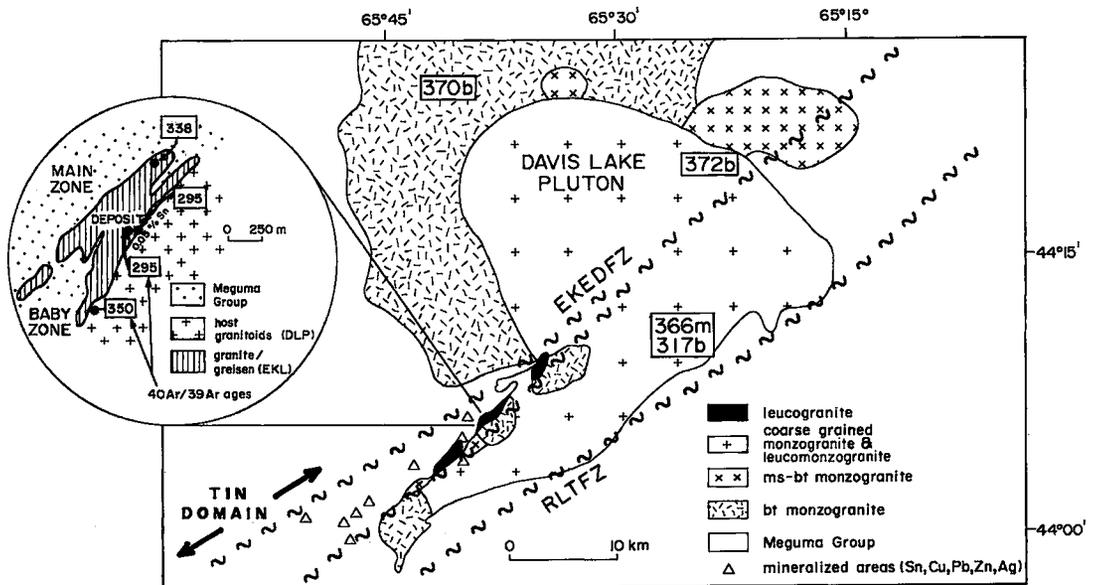

FIG. 2. Geology of the Davis Lake pluton [after MacDonald et al. (1989, Fig. 1) and Ham & MacDonald (1991)] and inset map of the East Kemptville deposit area [after Richardson et al. (1982), Fig. 4.2)]. The age data shown are $^{40}Ar/^{39}Ar$ plateau ages for mica (b, biotite; m, muscovite) from the Davis Lake pluton (from Reynolds et al. 1981) and $^{40}Ar/^{39}Ar$ plateau ages for muscovite from the East Kemptville deposit area [leucogranite and greisen; Zentilli & Reynolds (1985) and Kontak & Cormier (1991)]. The fault zones shown are the Rushmere Lake – Tobeatic Fault Zone (RLTFZ) and the East Kemptville – East Dalhousie Fault Zone (EKEDFZ). EKL and DLP in the inset map refer to East Kemptville leucogranite and Davis Lake pluton, respectively.

TABLE 1. GEOCHRONOLOGICAL DATA FOR THE EAST KEMPTVILLE LEUCOGRANITE AND GREISENS

Method	Source	Material	Age (Ma)	Comment[a]
$^{40}Ar/^{39}Ar$	1	Muscovite (N = 2, greisen)	300	Deformed greisens; dating of tectonothermal event
$^{40}Ar/^{39}Ar$	1	Muscovite (EKL)	~350	Sample of EKL marginal to deposit (Fig. 2); disturbed age spectrum, but 60% of gas indicates an age of ca. 350 Ma
$^{40}Ar/^{39}Ar$	2	Muscovite (EKL)	338	Sample of EKL from deposit area; disturbed age spectrum, but 66% of gas gives plateau age of 338 Ma
Rb/Sr	2	Whole rock (EKL)	344 ± 5	Isochron (MSWD = 1.26; N = 11); Sr_i = 0.7245 ± 0.0056; represents time of Rb/Sr rehomogenization due to tectonothermal event
Rb/Sr	2	Whole rock minus muscovite (EKL)	354 ± 13	Errorchron (MSWD = 9.0; N = 9); Sr_i = 0.7215 ± 0.0107; minimum age for leucogranite and time of rehomogenization of Rb/Sr
Rb/Sr	2	Muscovites (EKL)	320 ± 4	Isochron (MSWD = 3.0; N = 7); Sr_i = 0.7519 ± 0.0320; explanation remains ambiguous
Rb/Sr	2	WRMMS-QP-KF (EKL)	254 ± 23	Average of seven 3-point isochrons; low temperature resetting event
Rb/Sr	2	WRMMS-WR-MS	361-311	Range of ages (N = 7) reflecting variable resetting of WR-MS Rb/Sr isotopic system
Rb/Sr	3	Whole rock (greisen)	337 ± 5	Errorchron (MSWD = 2.87, N = 5); Sr_i = 0.729 ± 0.001; time of tectonothermal activity and resetting (cf. Richardson *et al.*, 1988)
Rb/Sr	4	Whole rock (EKL)	333 ± 27	Errorchron (MSWD = 12, N = 6); Sr_i = 0.724 ± 0.020; represents time of rehomogenization (cf. Richardson, 1988)
Pb/Pb	5	whole rocks (EKL and greisen) and mineral separates (MS, KF)	366 ± 4	Age of EKL intrusion and associated mineralization
U/Pb	5	whole rock (EKL and greisens)	367 ± 10	Age of EKL intrusion and associated mineralization

NOTES: Sources: 1 Zentilli & Reynolds (1985); 2 Kontak & Cormier (1991); 3 Richardson *et al.* (1988); 4 Richardson (1988); 5 Kontak & Chatterjee (1992); Sr_i, initial $^{87}Sr/^{86}Sr$ ratio; EKL, East Kemptville leucogranite; WRMMS, whole rock minus muscovite; QP, quartz-plagioclase fraction; KF, K-feldspar; WR, whole rock; MS, muscovite.
[a]Represents interpretation of the date by the authors.

Keppie & Dallmeyer 1987). Continued tectonothermal activity within the Meguma Terrane, albeit more localized in nature, is recorded by: (1) zones of brittle to ductile faulting that cross-cut the peraluminous granites (Fig. 2; Smith 1985, MacDonald *et al.* 1992, Horne *et al.* 1992), and (2) variably reset isotopic systems (Keppie & Dallmeyer 1987, Dallmeyer & Keppie 1987, Reynolds *et al.* 1987, Cormier *et al.* 1988, Kontak & Cormier 1991).

At East Kemptville, a topaz–muscovite leucogranite of <1 km² intrudes fine- to medium-grained, grey to black psammites of the Meguma Group. This granite represents the late-stage differentiate of the zoned Davis Lake pluton (MacDonald *et al.* 1992). The pluton has been dated at *ca.* 370 Ma based on a whole-rock Rb/Sr isochron (374 ± 5 Ma, *n* = 32; Chatterjee & Cormier 1991) and $^{40}Ar/^{39}Ar$ mica dating of mica (Reynolds *et al.* 1981, J.D. Keppie, pers. comm.,

1993). The leucogranite is fine- to medium-grained and varies from relatively fresh, with variable amounts of deuteric alteration, to intensely altered equivalents in areas of greisen and vein mineralization (Kontak 1990, 1991). However, all rocks record variable amounts of deformation, and one observes in outcrop the presence of a well-developed northeast-trending (generally 040°/45–75°NE) *S* fabric and, more rarely, mylonitic zones (1–2 meters in width) of similar orientation (Kontak *et al.* 1986, Kontak & Cormier 1991). Examination of deformed leucogranite in thin section reveals the following features: (1) recrystallization of quartz and development of undulatory extinction, (2) fracturing of grains of feldspar and displacement of albite twin planes, (3) inversion of orthoclase to maximum microcline, and (4) alignment and kinking of mica flakes and formation of through-going zones of deformation defined by recrystallized textures and

fine-grained white mica. Kontak (1990) and Kontak & Cormier (1991) interpreted the geological features of the area and the complex tectonothermal evolution to reflect emplacement of the leucogranite into an active fault-zone, represented today by the EKEDFZ (Fig. 2), which initially localized the intrusion and subsequently focused strain during continued deformation within the Meguma Terrane.

PREVIOUS GEOCHRONOLOGICAL STUDIES AND IMPLICATIONS FOR THE THERMAL HISTORY OF THE EAST KEMPTVILLE LEUCOGRANITE

Previous geochronological work at East Kemptville (Table 1) indicates that both emplacement of the leucogranite and associated hydrothermal activity occurred at 366 Ma (Pb/Pb, U/Pb). However, final closure of the whole-rock Rb/Sr system did not occur until 344 Ma, at about the same time as the oldest of four $^{40}Ar/^{39}Ar$ dates for muscovite (350 Ma). A minimum temperature of *ca.* 350°C is estimated for the latter thermal event, on the basis of Ar diffusivity in muscovite (McDougall & Harrison 1988). These data do not permit one to distinguish between a short-lived *versus* a protracted thermal event; however, the geological setting of the batholith (MacDonald *et al.* 1992) and additional geochronological data in this area (Reynolds *et al.* 1981, 1987) suggest a short-lived event. Concordant to discordant $^{40}Ar/^{39}Ar$ age spectra for the three remaining muscovite separates from East Kemptville, with plateau ages for part of the spectra of 338 Ma to 295 Ma, indicate variable thermal histories or steep thermal gradients in the region. A similar scenario is suggested on the basis of variable whole-rock – mineral Rb/Sr ages, as seven whole-rock – muscovite ages vary from 361 to 311 Ma, and seven whole-rock – plagioclase – K-feldspar ages vary from 276 to 240 Ma (Table 1). Although precise estimates of blocking temperatures for Rb/Sr systems are lacking, the highly different rates of diffusion of these elements in mica *versus* feldspar (Giletti 1991) would correspondingly translate into different blocking temperatures. For our purposes, it suffices to note that the large spread in Rb/Sr ages for similar whole-rock – mineral
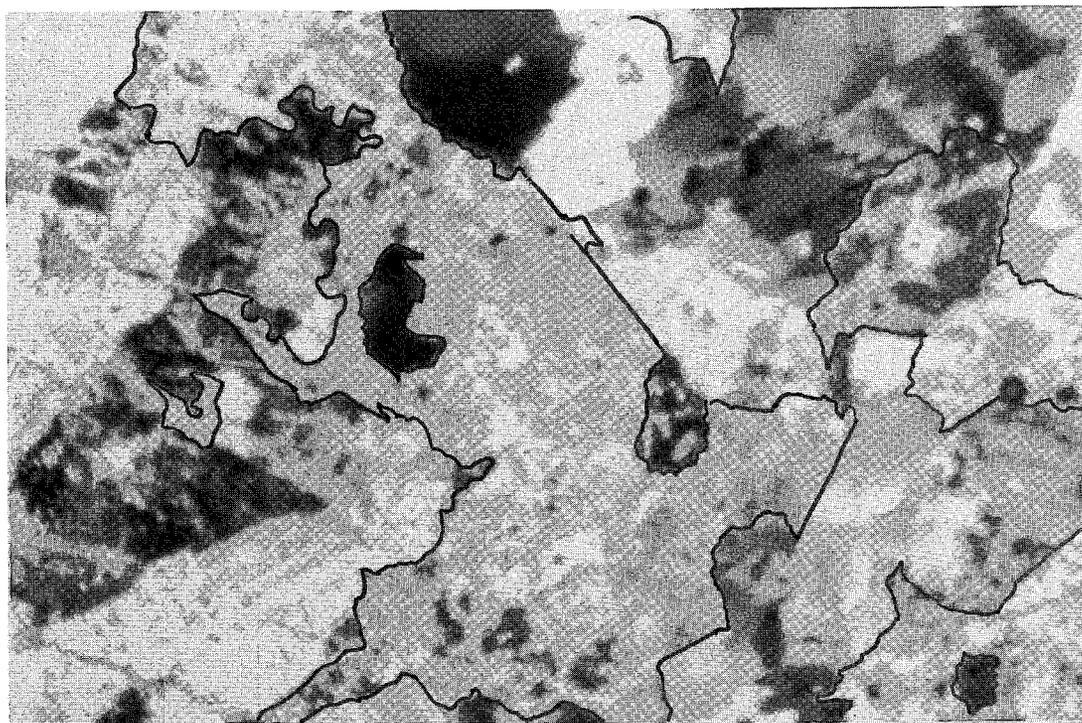

FIG. 3. Photomicrograph (crossed nicols) of sample EK–90–A showing muscovite grains (outlined in black ink). Muscovite grains are characterized by irregular terminations, internal recrystallization (*i.e.*, subgrain development) and kink zones. The large central grain consists mostly of a single, anhedral flake of muscovite, but the remaining areas consist of variably recrystallized and deformed muscovite and also aggregates of fine-grained muscovite. Width of photo is approximately 6 mm.

pairs must reflect variable thermal histories of the samples. In summary, previous work at East Kemptville indicates that separate thermal events have variably reset isotopic systems over a protracted time-interval and that the temperature accompanying these events must in some areas have approached *ca.* 350°C, the blocking temperature of muscovite.

SAMPLE SELECTION, DESCRIPTION AND ANALYTICAL TECHNIQUES

A single sample (EK–90–A) of barren, medium-grained, equigranular leucogranite (approximately 10 kg), characterized by a poorly developed spaced fracture-cleavage (040°/45°NE), was collected from the East Kemptville open pit (94 level, south end, summer 1990). In thin section, the rock contains no through-going fractures and has a hypidiomorphic-granular texture (Fig. 3). The petrography of the sample is similar to that of the leucogranite described by Kontak (1990), but we emphasize here the lack of obvious deformation. There is, however, subtle development of undulose extinction and sutured grain-boundaries in quartz, fracturing of the sodic plagioclase, and kinking of muscovite. Muscovite flakes are anhedral to sub-hedral, commonly with feathered or ragged termina-tions; kink zones transect grains, and subgrain development is not uncommon. In terms of grain size, muscovite occurs as coarse (500 to 1500 μm) to fine (<<500 μm) grains; the coarser grain-size dominates volumetrically (Fig. 4). The muscovite is interpreted to reflect both a primary magmatic generation (with later chemical equilibration); however, there is no evidence in this sample of a later tectonic stage (*i.e.*, neomorphic muscovite), which would have led to aligned grains of muscovite (*e.g.*, West & Lux 1993).

The leucogranite sample was pulverized in a jaw crusher, and the material sieved to recover several size-fractions (–40/+50, –50/+60, –60/+70, –70/+80,

–80/+100, –100/+120, –120/+140; Fig. 5). The amount of crushing done was minimized so as to preserve as much as possible the original dimensions of the muscovite grains in the rock. High-purity mineral separates were prepared using conventional techniques (Franz isodynamic separator, heavy liquids, hand picking); petrographic examination of the separates indicates an approximate purity of 99.9%. Measure-ments (*n* in the range 50 to 55) of the size of individual grains within the various size-fractions indicate the following results (avg. ± 1σ): –40/+50 (547 ± 109 μm), –50/+60 (473 ± 113 μm), –70/+80 (342 ± 68 μm), –80/+100 (310 ± 53 μm), –100/+120 (251 ± 51 μm), –120/+140 (173 ± 30 μm). Small aliquots of each mesh size were used for electron-microprobe analysis, X-ray-diffraction studies and $^{40}Ar/^{39}Ar$ dating.

Electron-microprobe analyses were done using a JEOL 733 Superprobe equipped with an Oxford Link EXL Energy Dispersion system at Dalhousie University using the following operating conditions: accelerating voltage 15 kV, sample current 10 nA, beam diameter 1 μm, and counting time 40 seconds. Instrument calibration was done on pure metal standards, and data reduction of raw counts was done using Link's ZAF matrix-correction program. Intralaboratory standards were run to check for preci-sion and accuracy. Representative compositions are presented in Table 2.

For the X-ray-diffraction study, a small amount (~10 mg) of the finest and of the coarsest fraction of the muscovite separated from sample EK–90–A was ground briefly in a mortar and pestle, so as not to induce structural damage. An internal standard (synthetic spinel, $MgAl_2O_4$) was mixed in with the muscovite. A paste was prepared with this mixture and silicone-based stopcock grease. The paste was spread on a piece of tape on the sample mount intended for the transmission-mode Guinier–Hägg focussing powder-diffraction camera (CuKα$_1$ radiation). The paste was
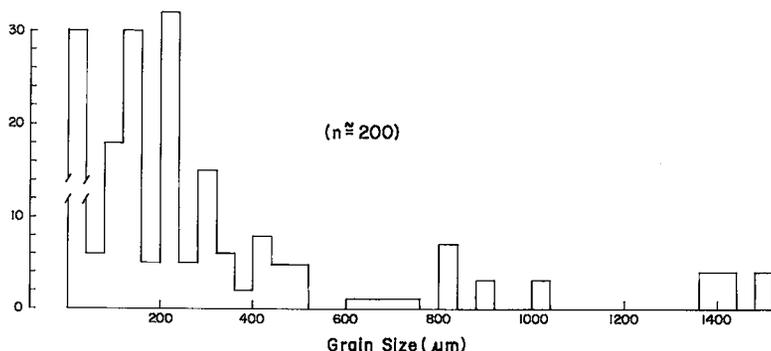

FIG. 4. Histogram plot of maximum dimensions of muscovite grains measured in thin section of leucogranite sample EK–90–A.
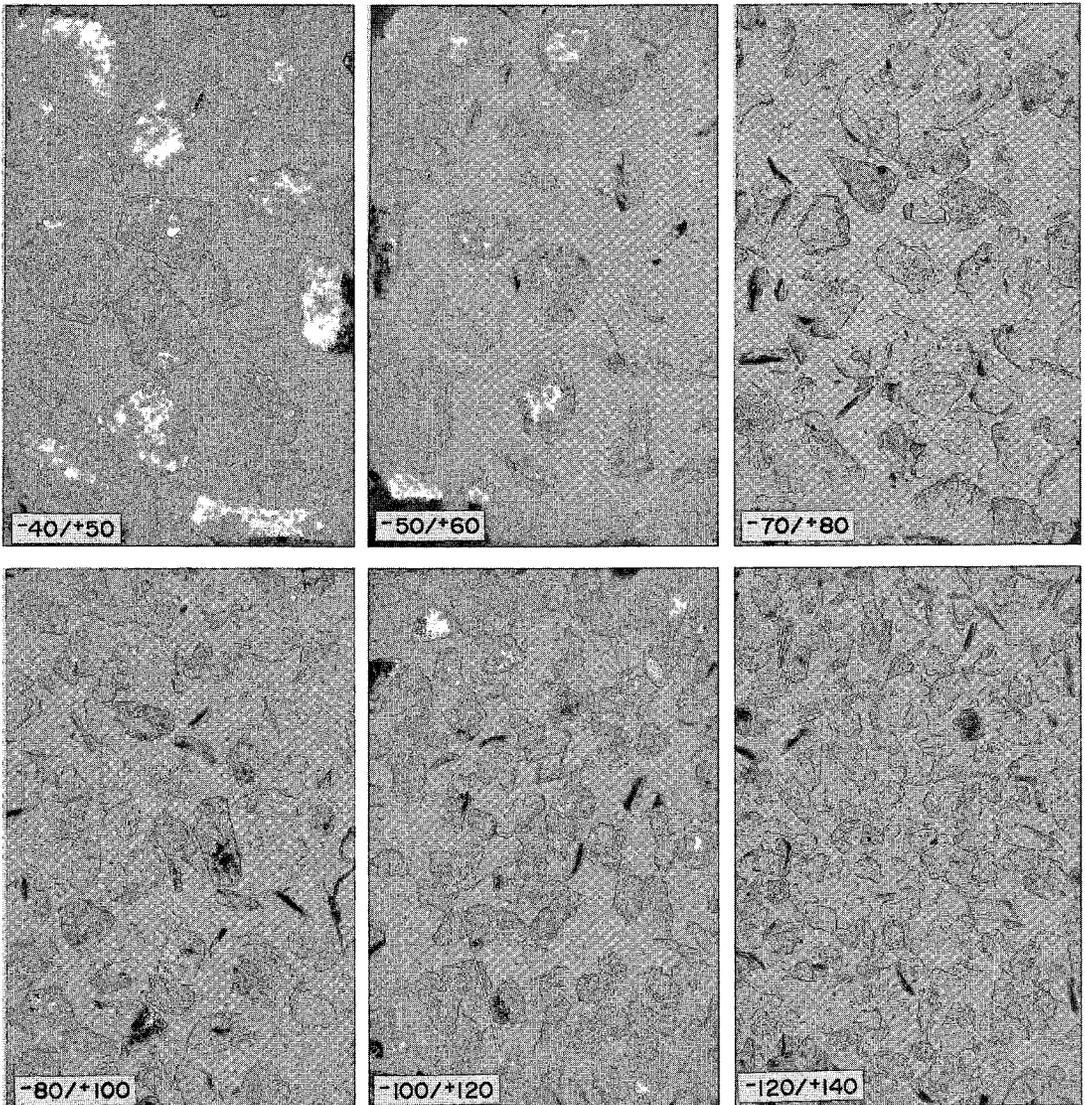
FIG. 5. Photomicrographs (plane-polarized light) of various size-fractions of muscovite; all photos have the same scale (long dimension 2.6 mm). Note that there are essentially two types of grains present, pitted grains full of inclusions and clear grains (see text for discussion). The dark spots in some grains reflect radiation haloes related to uraninite and zircon micro-inclusions.

spread with a minimum of manipulation, so as to minimize the preferred orientation of flakes in the paste. The diffraction patterns were indexed by reference to patterns for the polytypes of muscovite. The cell parameters of the two subsamples, refined with the program of Appleman & Evans (1973) as modified by Garvie (1986), are listed in Table 3.

Samples for $^{40}Ar/^{39}Ar$ analysis and several flux monitors were irradiated with fast neutrons at the

McMaster University Nuclear Reactor (Hamilton, Ontario) for 10 hours. The flux monitor used was the hornblende standard MMHb-1, which has an apparent K–Ar age of 519 Ma (Alexander et al. 1978), and each monitor was analyzed in two to four splits to check the uncertainty (0.7%) or reproducibility of the standard. J values derived from the analysis of the flux monitors formed a linear array when plotted as a function of position in the canister, indicating no detectable

TABLE 2. REPRESENTATIVE COMPOSITIONS OF THE VARIOUS SIZE–FRACTIONS OF MUSCOVITE
TAKEN FROM SAMPLE EK–90–A, EAST KEMPTVILLE LEUCOGRANITE

Mesh #	40/50 1	40/50 13	50/60 25	50/60 29	70/80 39	70/80 45	80/100 60	80/100 65	100/120 88	100/120 101	120/140 76	120/140 81
SiO_2	47.36	48.09	47.87	49.91	48.49	48.75	47.29	48.09	46.89	47.26	45.84	48.32
TiO_2	0.00	0.35	0.02	0.26	0.23	0.28	0.00	0.07	0.11	0.20	0.28	0.38
Al_2O_3	30.50	24.92	29.85	23.73	26.70	25.53	31.73	28.94	31.06	26.00	28.53	25.61
FeO	5.98	8.49	5.87	8.46	7.65	8.33	4.98	6.21	4.74	7.67	7.74	7.94
MnO	0.49	0.15	0.27	0.00	0.25	0.29	0.39	0.34	0.18	0.27	0.43	0.20
MgO	0.00	0.36	0.27	0.38	0.37	0.32	0.11	0.21	0.21	0.31	0.10	0.35
CaO	0.00	0.00	0.00	0.00	0.00	0.05	0.00	0.10	0.00	0.00	0.00	0.06
Na_2O	0.30	0.27	0.17	0.21	0.10	0.16	0.18	0.12	0.14	0.16	0.33	0.08
K_2O	9.67	10.11	9.59	9.83	9.69	9.62	9.41	9.70	10.96	10.81	10.57	10.77
F	1.86	3.45	1.75	4.05	2.89	3.29	1.67	2.36	1.60	3.24	2.48	3.39
Cl	0.00	0.00	0.00	0.00	0.00	0.05	0.00	0.03	0.00	0.07	0.00	0.03
	96.18	96.24	95.69	96.86	96.41	96.67	95.84	96.10	95.94	96.03	96.34	97.17
Cl,F=O	0.78	1.44	0.73	1.70	1.21	1.38	0.70	0.99	0.67	1.37	1.04	1.42
Σ	95.40	94.80	94.96	95.16	95.20	95.29	95.14	95.11	95.27	94.66	95.30	95.75

STRUCTURAL FORMULAE BASED ON 11 ATOMS OF OXYGEN

Si	3.245	3.407	3.283	3.507	3.375	3.410	3.219	3.315	3.214	3.354	3.220	3.382
^{IV}Al	0.755	0.593	0.717	.493	0.625	0.590	0.781	0.685	0.786	0.646	0.780	0.618
^{VI}Al	1.709	1.488	1.696	1.472	1.566	1.515	1.765	1.667	1.724	1.530	1.582	1.495
Ti	0.000	0.019	0.001	0.014	0.012	0.015	0.000	0.004	0.006	0.011	0.015	0.02
Fe^{2+}	0.341	0.503	0.337	0.497	0.446	0.487	0.284	0.358	0.272	0.456	0.455	0.465
Mn	0.033	0.009	0.016	0.000	0.015	0.017	0.023	0.020	0.011	0.017	0.026	0.012
Mg	0.000	0.039	0.028	0.040	0.039	0.034	0.011	0.022	0.022	0.033	0.011	0.037
Ca	0.000	0.000	0.000	0.000	0.000	0.000	0.004	0.000	0.000	0.000	0.000	0.004
Na	0.044	0.038	0.023	0.030	0.015	0.022	0.024	0.016	0.020	0.022	0.045	0.012
K	0.847	0.914	0.839	0.882	0.861	0.859	0.818	0.853	0.959	0.979	0.948	0.962
F	0.407	0.775	0.380	0.902	0.637	0.729	0.360	0.515	0.347	0.728	0.552	0.750
Cl	0.000	0.000	0.000	0.000	0.000	0.007	0.000	0.004	0.000	0.008	0.000	0.004

Concentrations of oxides in wt.% as determined by electron–microprobe analysis using the following operating conditions: accelerating voltage 15 kV, sample current 10 nA, beam width 1 μm, counting time 40 seconds. Reduction of data done using Link's ZAF matrix–correction program.

gradient in the neutron flux for this position. For $^{40}Ar/^{39}Ar$ incremental step-heating experiments, samples were loaded into a quartz tube connected to a stainless-steel extraction system and heated using a Lindberg furnace. The extraction system was operated on-line to a substantially modified AEI MS–10 mass spectrometer run in the static mode. Measured mass-spectrometric ratios were extrapolated to zero-time and corrected to an $^{40}Ar/^{36}Ar$ atmospheric

ratio of 295.5. The $^{40}Ar/^{39}Ar$ values were corrected for neutron-induced ^{40}Ar from potassium and ^{39}Ar and ^{36}Ar from calcium. Ages and errors were calculated using formulae given by Dalrymple et al. (1981) and the constants recommended by Steiger & Jäger (1977). The errors represent the analytical precision at 2σ, assuming that the error in the J-value is zero. The results are summarized in Tables 4 and 5.

PETROGRAPHY AND MINERAL CHEMISTRY
OF THE SIZE FRACTIONS OF MUSCOVITE

Photomicrographs of the size fractions of muscovite are shown in Figure 5; the representative compositions of the size fractions (Table 2) are summarized in Figure 6. The muscovite grains can be crudely subdivided into two categories on the basis of their texture, namely pitted and clear types. The pitted types are characterized by the presence of a variety of mineral inclusions of various sizes, shapes and abundance. On the basis of back-scattered electron (BSE) imaging and semiquantitative energy-dispersion analysis (EDS), these include pyrite, chalcopyrite, galena, sphalerite, native bismuth, uraninite, cassiterite, Nb–Ta oxides,

TABLE 3. UNIT–CELL PARAMETERS OF MUSCOVITE
IN THE FINEST AND COARSEST SIZE–FRACTIONS,
SAMPLE EK–90–A, EAST KEMPTVILLE LEUCOGRANITE

	a	b	c	α	β	γ	V	#
–40/+50 mesh	5.2108 0.0007	9.0609 0.0015	19.9965 0.0064	90	95.800 0.018	90	939.62 0.27	33
–120/+140 mesh	5.2145 0.0012	9.0580 0.0019	20.0056 0.0103	90	95.740 0.031	90	940.18 0.45	35

number of indexed peaks used in the least–squares refinement [program of Appleman & Evans (1973), as adapted by Garvey (1986)]. Units: a, b, c in Å, and V (unit–cell volume) in Å^3; interaxial angles in direct and reciprocal space in degrees. End–member muscovite–$2M_1$ (PDF 6–263) has the following unit–cell parameters: a 5.19, b 9.03, c 20.05 Å, β 95.77°.

TABLE 4. $^{40}Ar/^{39}Ar$ EXPERIMENTAL DATA FOR THE VARIOUS SIZE–FRACTIONS OF MUSCOVITE TAKEN FROM SAMPLE EK–90–A, EAST KEMPTVILLE LEUCOGRANITE

	Temp °C	$^{40}Ar/^{39}Ar$	$^{36}Ar/^{39}Ar$	$^{37}Ar/^{39}Ar$	Vol. 10-8 cm³	Fraction ^{39}Ar	$\%^{40}Ar$ Rad.	Age Ma	± Error 2 sigma
C-6	600	116.613	0.0972	0.000	0.257	0.021	75.37	337.3	3.5
	675	80.830	0.0151	0.000	0.700	0.057	94.50	296.6	1.7
	730	76.882	0.0053	0.000	0.632	0.051	97.98	292.8	1.0
	770	77.324	0.0048	0.000	0.693	0.056	98.16	294.8	1.2
	810	79.281	0.0037	0.000	1.335	0.108	98.63	303.1	1.2
	840	81.482	0.0036	0.000	1.630	0.132	98.71	311.0	0.7
	870	84.118	0.0059	0.000	1.849	0.149	97.94	317.9	1.5
	*910	85.563	0.0012	0.000	3.854	0.311	99.59	327.9	0.5
	*960	87.003	0.0067	0.000	0.753	0.061	97.71	327.2	2.9
	*1050	87.545	0.0101	0.000	0.226	0.018	96.58	325.6	2.9
	1200	86.079	0.0112	0.000	0.451	0.036	96.14	319.3	2.4
C-7	600	100.010	0.0839	0.000	0.229	0.017	75.20	292.4	9.5
	680	79.887	0.0137	0.000	0.693	0.051	94.93	294.6	1.4
	735	75.983	0.0078	0.000	0.707	0.052	96.98	286.9	2.5
	775	76.967	0.0050	0.000	0.832	0.062	98.07	293.3	1.8
	815	79.638	0.0044	0.000	1.723	0.128	98.38	303.6	1.6
	845	81.387	0.0036	0.000	2.112	0.157	98.70	310.6	2.2
	*875	84.820	0.0027	0.000	3.539	0.263	99.07	323.8	1.6
	*905	86.631	0.0080	0.000	1.999	0.149	97.26	324.5	2.3
	950	86.703	0.0037	0.000	0.816	0.061	98.73	329.3	2.1
	1050	85.203	0.0102	0.000	0.372	0.028	96.46	317.2	2.7
	1200	84.147	0.0170	0.000	0.442	0.033	94.02	306.3	3.0
C-8	600	73.988	0.0152	0.000	0.774	0.059	93.92	271.7	4.5
	680	75.574	0.0045	0.000	1.124	0.085	98.25	288.9	1.2
	735	75.931	0.0043	0.000	0.910	0.069	98.34	290.4	2.3
	775	79.194	0.0067	0.000	0.906	0.069	97.49	299.5	1.8
	815	81.557	0.0044	0.000	1.800	0.137	98.42	310.4	1.6
	845	84.735	0.0040	0.000	2.700	0.205	98.61	322.1	2.1
	*875	87.030	0.0042	0.000	2.409	0.183	98.56	329.9	2.7
	*905	87.013	0.0042	0.000	1.483	0.113	98.57	329.9	1.7
	*950	87.212	0.0049	0.000	0.566	0.043	98.35	329.9	1.6
	1050	88.155	0.0171	0.000	0.211	0.016	94.28	320.5	2.5
	1200	88.189	0.0201	0.000	0.278	0.021	93.25	317.4	3.7
C-9	600	88.133	0.0353	0.000	0.369	0.028	88.18	301.33	4.1
	680	79.720	0.0123	0.000	0.758	0.057	95.45	295.5	1.8
	735	77.594	0.0066	0.000	0.733	0.055	97.47	239.9	2.3
	775	79.621	0.0083	0.000	0.823	0.062	96.92	299.4	2.7
	815	81.631	0.0057	0.000	1.587	0.120	97.93	309.3	3.2
	845	83.680	0.0041	0.000	2.637	0.199	98.55	318.2	1.9
	*875	86.507	0.0049	0.000	3.020	0.228	98.32	327.3	2.0
	*905	85.739	0.0030	0.000	1.373	0.104	98.97	326.6	1.4
	950	86.706	0.0029	0.000	1.256	0.095	99.01	330.2	1.9
	1050	87.299	0.0066	0.000	0.417	0.032	97.75	328.3	2.8
	1200	89.829	0.0217	0.000	0.248	0.019	92.86	321.6	3.6
C-10	600	95.198	0.0481	0.000	0.351	0.028	85.08	313.0	3.1
	680	80.055	0.0127	0.000	0.796	0.062	95.30	296.2	2.6
	735	77.499	0.0061	0.000	0.776	0.061	97.68	294.1	1.5
	775	79.163	0.0061	0.000	0.848	0.067	97.72	300.1	2.2
	815	81.227	0.0041	0.000	1.835	0.144	98.52	309.6	2.4
	845	84.310	0.0042	0.000	2.580	0.202	98.52	320.3	2.1
	*875	85.746	0.0035	0.000	2.388	0.187	98.78	326.1	1.2
	*905	85.674	0.0031	0.000	1.842	0.144	98.92	326.3	1.4
	950	86.839	0.0032	0.000	0.885	0.069	98.90	330.3	0.8
	1050	88.088	0.0106	0.000	0.302	0.024	96.43	327.0	3.6
	1200	95.238	0.0450	0.000	0.144	0.011	86.04	316.4	3.9
C-11	600	65.400	0.0230	0.000	0.566	0.043	89.59	231.7	1.2
	680	77.148	0.0078	0.000	0.974	0.074	97.01	291.0	2.7
	735	76.228	0.0045	0.000	0.789	0.060	98.24	291.2	2.4
	775	78.701	0.0055	0.000	0.918	0.070	97.95	299.1	2.2
	815	81.073	0.0048	0.000	1.620	0.123	98.25	308.2	1.0
	845	83.588	0.0050	0.000	2.866	0.218	98.23	316.9	1.6
	*875	85.883	0.0039	0.000	2.329	0.177	98.67	326.3	0.9
	*905	85.565	0.0044	0.000	1.660	0.126	98.47	324.6	1.8
	950	86.665	0.0044	0.000	0.920	0.070	98.49	328.4	0.9
	1050	87.043	0.0093	0.000	0.369	0.028	96.84	324.7	1.1
	1200	93.530	0.0462	0.000	0.122	0.009	85.40	309.0	3.5
C-12	600	86.942	0.0487	0.000	0.245	0.017	83.46	282.8	3.7
	680	77.355	0.0081	0.000	1.002	0.071	96.91	291.5	1.5
	735	75.912	0.0050	0.000	0.854	0.060	98.05	289.6	1.7
	775	77.571	0.0057	0.000	0.892	0.063	97.83	294.8	3.1
	815	80.420	0.0048	0.000	1.905	0.135	98.22	305.9	1.3
	845	81.995	0.0046	0.000	2.573	0.182	98.35	311.8	1.0
	*875	88.258	0.0145	0.000	3.252	0.230	95.15	323.6	2.6
	*905	89.445	0.0176	0.000	2.225	0.157	94.18	324.5	1.1
	*950	85.818	0.0046	0.000	0.850	0.060	98.43	325.3	2.9
	*1050	87.448	0.0111	0.000	0.258	0.018	96.24	324.2	2.2
	1200	95.980	0.0547	0.000	0.099	0.007	83.16	308.8	9.0

* Denotes steps used to calculate plateau ages in Figure 8 and Table 5, as discussed in the text.

niobian rutile, apatite, triplite, monazite and zircon. The pitted grains commonly have a texture similar to the sagenitic texture seen in biotite; it possibly is due to a fine-grained, lamellar intergrowth of rutile. In contrast, the clear grains are devoid of inclusions, but otherwise seem the same with respect to their morphology and birefringence. Both types contain kink bands, undulatory extinction and some intragranular recrystallization, suggesting that they have experienced the same complex evolution.

The various size-fractions of muscovite have a large range in composition, mostly in the proportions of Fe, Si, Al and F; histograms in Figure 6 illustrate the broad overlap of the composition for each of these size fractions. The elemental variations in muscovite from this single sample are the same as documented in muscovite from the leucogranite and greisens (Kontak 1991, 1994). The broad variation in chemistry can also be documented within single grains; this is particularly notable with respect to Fe contents, as illustrated by a BSE image of a muscovite grain in Figure 7. In this image, the light portions, which represent areas with higher average atomic number, contain 7 to 9 wt.% FeO, whereas the darker areas have less than 5 wt.% FeO. Thus, the chemical variability occurs on an intra-grain scale and is not simply a function of grain size. The results of the mineral chemistry, in conjunction with petrographic observations, suggest that although muscovite is of variable morphology and chemistry, it may have formed in one of several manners: (1) initial crystallization of the leucogranitic magma, (2) crystallization as in (1) but with subsequent interaction with a hydrothermal fluid during deuteric alteration, or (3) formation during the hydrothermal stage, i.e., the muscovite is of postmagmatic origin.

RESULTS OF X-RAY-DIFFRACTION STUDIES

The X-ray-diffraction (XRD) studies of the coarsest and finest sizes-fractions (Table 3) showed that both the 40–50 and 120–140 mesh samples contain muscovite-$2M_1$. The two sets of cell dimensions differ slightly, and are within 2σ of each other. There is no evidence of significant compositional differences between the two size-fractions. The background of the films is darker than expected, which is consistent with the presence of Fe in the octahedral sites (phengitic component). In addition, the cell dimensions a and b are slightly larger than in end-member muscovite (Table 3, footnote), presumably reflecting the presence of Fe, whereas c is slightly smaller than expected, presumably because of the presence of significant fluorine at the hydroxyl site. Finally, and most importantly, the data do not indicate the presence of a polytype other than $2M_1$ in the samples examined.

Our results can be compared to the findings of Palmer (1991), who studied twelve samples of muscovite from East Kemptville. Palmer determined, with the use of a Debye–Scherrer camera, that all twelve samples consist of the muscovite-$2M_1$ polytype. He attributed the differences between the two populations (leucogranite versus greisen) to variations in the occupancy of the octahedral sites.

TABLE 5. SUMMARY OF $^{40}Ar/^{39}Ar$ STEP–HEATING EXPERIMENTS ON THE VARIOUS SIZE–FRACTIONS
OF MUSCOVITE TAKEN FROM SAMPLE EK–90–A, EAST KEMPTVILLE LEUCOGRANITE

Sample #	Size Fraction	%K[1]	Minimum Age (Ma)	Maximum Age (Ma)	Integrated Age (Ma)	Maximum[2] ^{39}Ar	Temp (°C) at Max. ^{39}Ar	Plateau Age	%^{39}Ar Plateau	# Steps Plateau
C6	40/50	7.5	292.8	337.3	315.9	3.85	910	327.7	39.0	3
C7	50/60	8.1	286.9	329.3	313.0	3.53	875	324.0	41.1	2
C8	60/70	7.9	288.9	329.9	313.5	2.70	845	329.9	33.9	3
C9	70/80	7.7	294.1	330.2	316.9	2.58	845	326.2	33.2	2
C10	80/100	8.0	293.9	330.3	317.3	3.02	875	327.1	33.2	2
C11	100/120	7.9	231.7	328.4	311.0	2.86	845	325.5	30.4	2
C12	120/140	8.5	282.8	325.3	312.4	3.25	905	324.1	46.5	4

[1]% K (expressed in wt. %) is approximated, based on the volume ^{39}Ar released and appropriate constants.
[2]Maximum volume ^{39}Ar (10^{-8} cm³) calculated for individual steps.
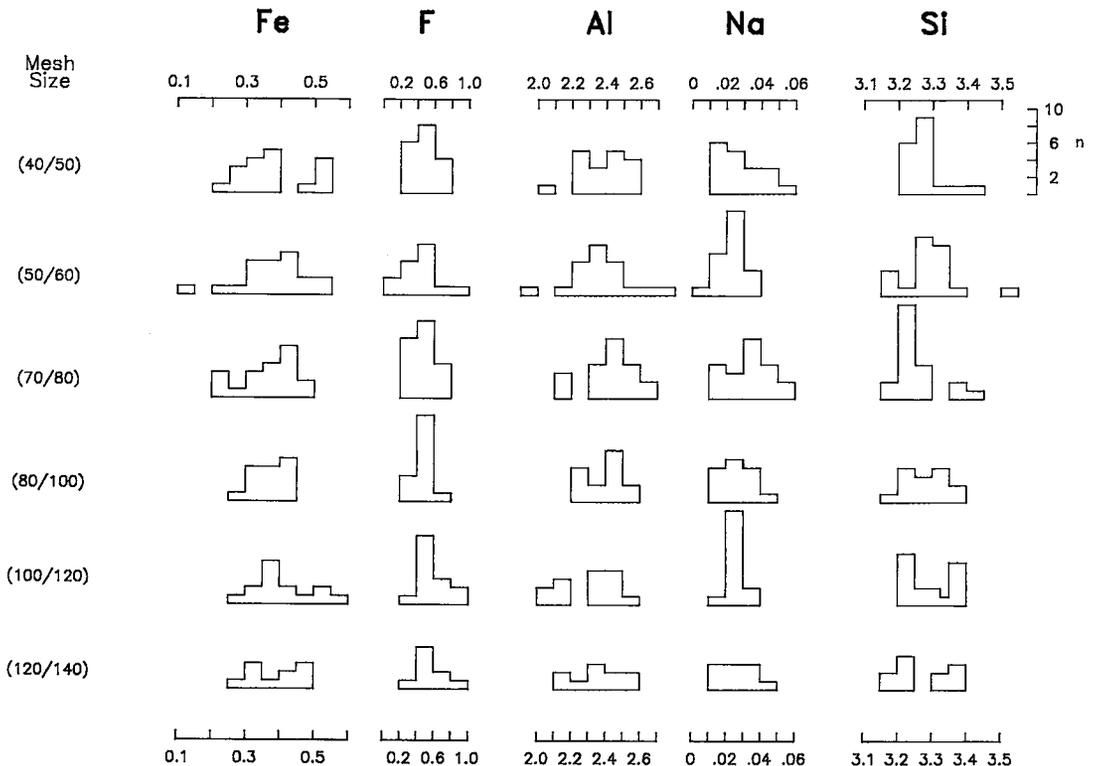
FIG. 6. Histograms summarizing the chemistry of muscovite for the various size-fractions. All data are given in atomic proportions based on 11 atoms of oxygen per formula unit.
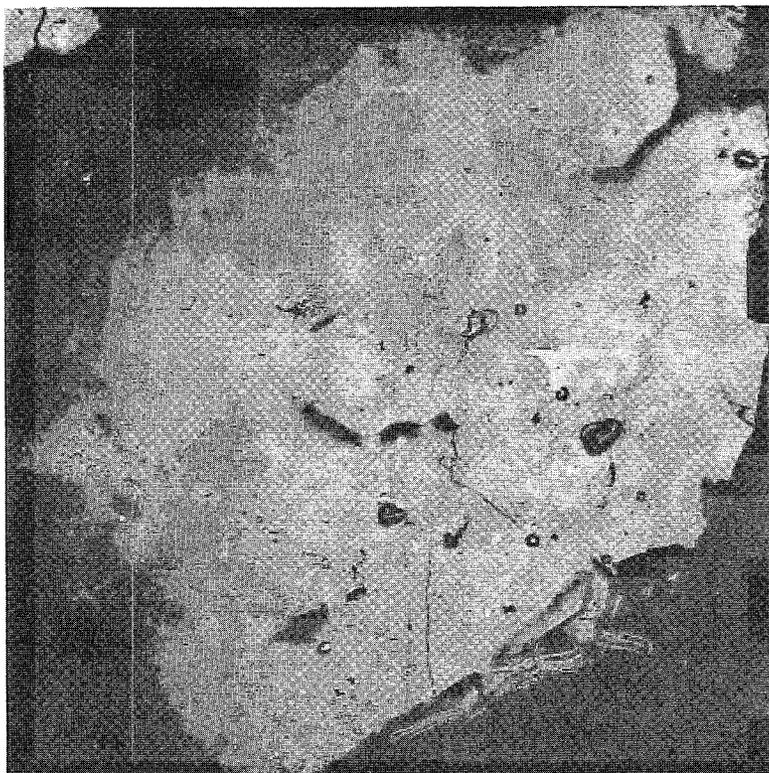
FIG. 7. Back-scattered electron image (BSE) of a muscovite grain from the –40/+50 mesh fraction. The variation in color (light *versus* dark patches) reflects the variation in average atomic number in the mineral, in this case the variation in proportion of Fe in the light (7–9 wt.% FeO) and dark (<5 wt.% FeO) areas. Note the irregular nature of the distribution of these zones, suggestive of a secondary (*i.e.*, postmagmatic) origin.

RESULTS OF ^{40}Ar/^{39}Ar INCREMENTAL STEP-HEATING EXPERIMENTS

The age spectra for seven incremental step-heating experiments are presented in Table 4 and Figure 8, and the important results are summarized in Table 5. For each sample, outgassing was performed using the same heating schedule ($n = 11$ steps) to ensure valid comparison among the size fractions. The results are remarkably uniform for all size fractions, with the following points noted: (1) similar values for minimum (with one exception), maximum and integrated ages, (2) similar gas-release patterns, as indicated in the plots of volume of gas liberated (represented as ^{39}Ar) *versus* temperature, and (3) comparable age spectra reflecting, therefore, similar distribution of ^{40}Ar within the size fractions.

Examination of the age spectra in more detail indicates that in all cases, samples are characterized by young ages for the low-temperature gas fractions, after which ages increase monotonically for successive steps, such that maximum ages are recorded for the high-temperature gas fractions. There occurs, however, in all samples a tailing off of the ages for the final 1–3% of the gas released, presumably reflecting outgassing of Ar from a relatively more retentive site. The low-temperature ages are generally uniform at 300 ± 20 Ma, except where either anomalously younger (C–11) or older (C–6) apparent ages were obtained. For sample C–11, the first step at 600°C has an anomalously low age of 231 Ma, but the subsequent two steps (680° and 735°C) have identical apparent ages of 291 Ma. Similarly, for sample C–6, the first step (600°C), with an age of 337 Ma, is succeeded by three steps with apparent ages of 292 to 296 Ma.

The results for the seven size-fractions are internally consistent, but differ from results for the four samples of muscovite previously analyzed (Zentilli & Reynolds 1985, Kontak & Cormier 1991) by step-heating experiments in terms of their profiles, plateau ages and
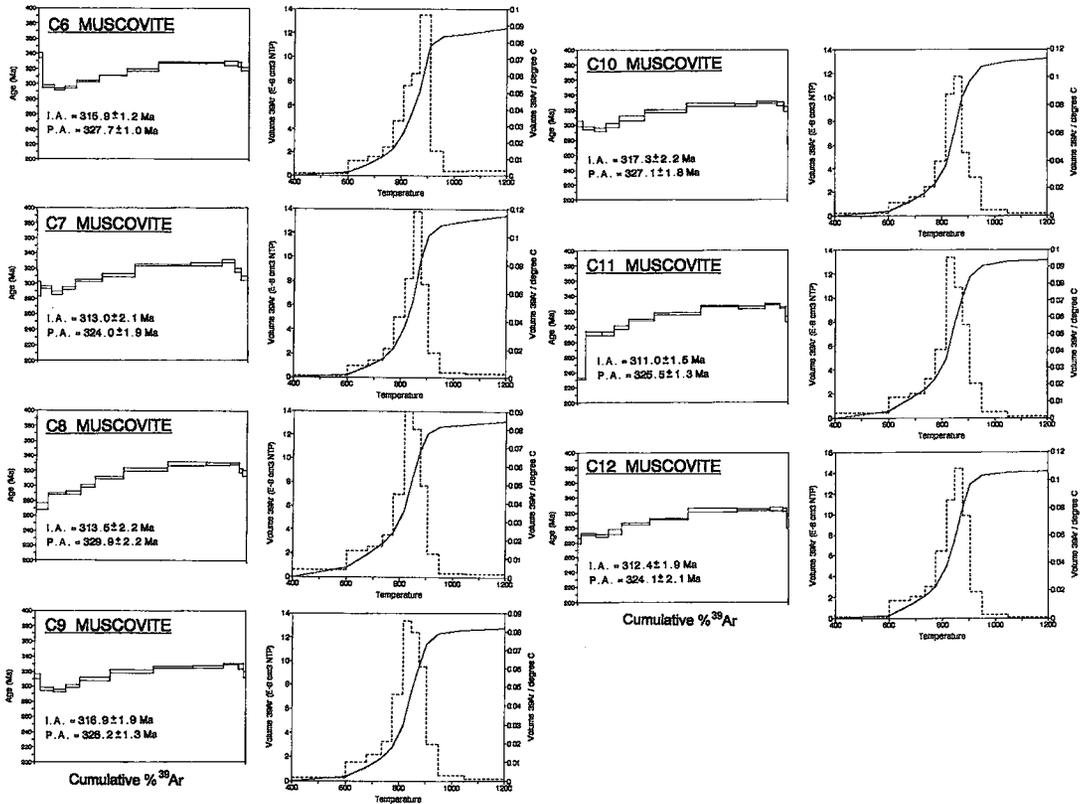
FIG. 8. Summary of ^{40}Ar/^{39}Ar age spectra for step-wise heating experiments conducted on the seven size-fractions of muscovite. The samples are ordered from the coarsest (C6, –40/+50) to the finest (C12; –120/+140) grain size. Abbreviations: I.A. = integrated age; P.A. = plateau age. For plateau segments (P.A.), the steps used are indicated by an asterisk in Table 4, but note that these are not strictly plateau ages, since in these segments less than 50% of the total gas released is included in the calculations. In the adjacent box diagrams, the dashed line shows the volume of ^{39}Ar (10^{-8} cm^3 NTP) for each step, whereas the solid line shows the volume ^{39}Ar/°C for each step.

integrated ages. The profiles obtained are most similar to the single age spectrum reported by Kontak & Cormier (1991), for which the low-temperature fractions of gas indicated apparent ages of 269 to 286 Ma, and the high-temperature steps indicated a plateau (62% gas released) age of 338 ± 2 Ma. The integrated age of this sample, 326 Ma, is older than the integrated ages for the fractions dated in this study (Table 5).

Discussion

The results of our crystal-chemical and step-heating experiments on muscovite from a single sample of leucogranite from East Kemptville provide information that can be used to interpret the complex geochronological evolution of this part of the Meguma Terrane. However, first it is necessary to address the role of various parameters that have influenced the age spectra

of the muscovite samples in order to discern which factors are the most important and to evaluate the significance of the apparent ages.

Patterns of regional cooling

On the basis of ^{40}Ar/^{39}Ar dating (Reynolds et al. 1981, Keppie et al. 1993, J.D. Keppie, pers. comm., 1993), whole-rock Rb/Sr (Chatterjee & Cormier 1991) and Pb–Pb (Chatterjee & Ham 1991) methods, regional cooling of the Davis Lake pluton to below ca. 350°C occurred at 370 Ma. For example, outside the fault zones, but within the pluton (Fig. 2), muscovite separates yield undisturbed ^{40}Ar/^{39}Ar release spectra that are identical to ca. 370 Ma whole-rock Rb/Sr and Pb–Pb isochron ages. If the resetting observed at East Kemptville was part of a regional thermal event analogous to differential postmetamorphic cooling, then a systematic pattern of varying mica ages should

be observed (e.g., Dallmeyer 1975, Harrison et al. 1989, West & Lux 1993); such is not the case. Instead, a broad area of consistent mineral ages is observed in the Davis Lake pluton, with younger ages observed within fault zones transecting the granite, as at East Kemptville. Thus, we conclude that neither slow cooling nor a regional reheating event can account for the discordant age spectra in the muscovite samples.

Cause of discordance in the muscovite samples

There are several aspects of the discordant age spectra for muscovite from East Kemptville that require consideration: (1) the origin of the apparent diffusive loss profiles in the various size-fractions analyzed, (2) the significance of the apparent ages obtained for the size fractions, and (3) the reason for the variability in spectra for the various samples analyzed within the deposit area. These aspects are evaluated in turn.

Origin of apparent diffusive-loss profiles

The origin of the diffusion-type profiles for the muscovite age spectra may reflect: (1) partial diffusive loss of radiogenic argon during a thermal event, (2) a mixture of different grain-sizes or presence of contaminants, (3) a mixture of muscovite polytypes, and (4) intragranular deformation during formation of the EKEDFZ.

In the first case, data discussed above suggest that the discordant age spectra are not related to partial diffusive loss of ^{40}Ar related to a regional thermal event after the initial cooling of the area through the argon blocking temperature, ca. 350°C (McDougall & Harrison 1988). Instead, the observation that discordant age spectra characterize samples collected from a fault zone (EKEDFZ, Fig. 2) suggests possible loss of radiogenic ^{40}Ar from the muscovite concurrent with the same tectonothermal event responsible for formation and re-activation of this structure.

A second possible explanation for the apparent diffusive-loss profile for the muscovite samples is related to mixed or contaminating phases of different ages. Wijbrans & McDougall (1986) and West & Lux (1993) have inferred such a model to account for the apparent diffusive profiles obtained in age studies of metamorphic rocks containing two distinct generations of muscovite, a coarse and fine fraction. In the case of the East Kemptville samples, there is no correlation of any measured parameter with grain size, as might be expected if paragenetically and temporally different grains of muscovite of various sizes were mixed. For example, West & Lux (1993) showed that both the shape of the age spectra and lower integrated ages characterize the finer grain-size fractions of muscovite in deformed rocks from a fault zone. These authors could relate this feature to the fact that fine-grained,

neomorphic muscovite grew late during formation of the fault zone. On the basis of petrographic observations that a distinct, later-generation muscovite of tectonic origin does not exist in sample EK–90–A, we conclude that the presence of a mixture of two distinct populations of muscovite of different age and different grain-size is not a plausible explanation of the age spectra.

As a third possible explanation, there could be a mixture of polytypes of muscovite, as found by Wijbrans & McDougall (1986, 1988), and Scaillet et al. (1992). It is not possible to model the age spectra by mixing the more retentive $3T$ polytype with the less retentive $2M_1$ polytype, as documented in studies of polythermal metamorphic terranes (e.g., Wijbrans & McDougall 1986, 1988), as we have shown that a single polytype occurs ($2M_1$). The composition of the muscovite in the size fractions is consistent with the cell parameters determined from refinement of the X-ray-diffraction data.

The fourth and final explanation, that of intragranular deformation of muscovite resulting in partial diffusive loss of argon, is difficult to assess; the sample was selected for its lack of deformational features. However, there is certainly petrographic evidence suggesting deformation of muscovite and partial development of subgrains within the coarser grains. Other samples within the deposit area, albeit from more strongly deformed areas, clearly demonstrate more extensive development of such features. The chemical heterogeneity within muscovite (Fig. 7) indicates the presence of distinct domains that would not be readily noticed in a routine petrographic examination.

Thus we conclude that the apparent diffusive-loss profiles for the muscovite samples are controlled by subgrain development due to a combination of both physical and chemical phenomena. The physical processes reflects the influence of the fault zone and its periodic reactivation over time, whereas the chemical effect reflects the inherent heterogeneity developed early owing to a combination of magmatic and hydrothermal processes. Since there is no notable difference in the age spectra for different grain-sizes, the effective grain-size controlling argon diffusivity must have been smaller than the smallest size-fraction analyzed (i.e., <175 μm).

Significance of apparent ages from $^{40}Ar/^{39}Ar$ age spectra

Both theoretical modeling (Turner 1968) and field-based studies (Hanson et al. 1975, Harrison & McDougall 1980, West & Lux 1993) show that the initial low-temperature gas increments in diffusive-loss profiles in $^{40}Ar/^{39}Ar$ age spectra are coincident with the time of the event that produced loss of radiogenic ^{40}Ar. Thus the minimum ages of ca. 300 Ma for the low-temperature gas fractions (Tables 4, 5) approximate

the time of the tectonothermal event. These ages are similar to the nearly concordant age spectra of 295 to 300 Ma obtained for two muscovite samples by Zentilli & Reynolds (1985). By analogy, the ages of the high-temperature gas fractions should give a minimum estimate of the original age of the sample. However, in this case, the ages of *ca*. 330 Ma are well below the inferred age of crystallization of the leucogranite, 370 Ma (Table 1). The potential significance of the 330 Ma age is discussed below.

Origin of variable $^{40}Ar/^{39}Ar$ age spectra within the East Kemptville area

Results of the present study, combined with previous work in the East Kemptville area, indicate a marked variation in the $^{40}Ar/^{39}Ar$ age spectra for muscovite. We have examined the most important factors generally considered to affect argon diffusivity and conclude that they have not been significant in terms of accounting for the observations. In light of these conclusions and additional geochronological data for the southwestern Meguma Terrane that document the presence of episodic tectonothermal events of Carboniferous and Permian age (Muecke *et al*. 1988, Dallmeyer & Keppie 1987, Cormier *et al*. 1988), we suggest that the variable age spectra reflect very localized structural focusing of heated fluids. This mechanism would result in the generation of steep thermal gradients that could account for the marked differences in age spectra over short lateral distances. The strong anisotropy within the rocks (*i.e*., deformation fabric) may be significant in this respect because it would provide a means of concentrating heated fluids along narrow structures or conduits (*i.e*., perhaps only tens of meters) within which partial resetting of muscovite phases occurred. An additional factor, but one that is difficult to quantify, is the extent of development of the subdomains within the muscovite grains, which will control the effective grain-size of argon diffusion.

Implications for the thermal history of the southwest Meguma Terrane

The new data presented here, in conjunction with results of previous geochronological studies of the East Kemptville (Table 1) and the surrounding area, invite some comments with regards to the thermal evolution of this part of the Meguma Terrane. As noted in Table 1, the emplacement of the leucogranite and related mineralization both occurred at *ca*. 370 Ma. However, less robust isotopic systems than U–Pb and Pb–Pb indicate considerably younger ages, with the maximum Rb–Sr whole-rock ages coinciding with the maximum $^{40}Ar/^{39}Ar$ muscovite age at about 350 Ma. Although a single temperature of closure does not exist as such for the whole-rock Rb–Sr system, a

temperature of *ca*. 350°C is sufficient to allow argon diffusion in muscovite (McDougall & Harrison 1988), and a slightly lower temperature (*ca*. 325°C) is suggested by Snee *et al*. (1988) if the muscovite consists of the $2M_1$ polytype. It is not possible, however, to distinguish between a protracted thermal event of about 20 Ma and a single tectonothermal event of short duration that would have had to completely homogenize the Rb–Sr systematics and reset the K–Ar system. The various Rb–Sr whole-rock – mineral and $^{40}Ar/^{39}Ar$ muscovite ages indicate that later thermal events were clearly of variable magnitude, causing in some cases complete resetting of muscovite (*e.g*., 300 Ma age spectra), whereas in others, only partial resetting (Fig. 8 of this study). Thus, temperatures associated with these episodic events must have fluctuated from close to that required to reset the muscovite K–Ar system to that causing only partial resetting.

CONCLUSIONS

Detailed $^{40}Ar/^{39}Ar$ step-heating experiments combined with crystal-chemical and XRD studies of seven grain-size fractions of muscovite from the East Kemptville leucogranite (366 Ma) indicate: (1) a similar mineral chemistry for all size fractions, (2) the presence of a single polytype of muscovite, $2M_1$, and (3) similar age spectra, with maximum and minimum apparent ages of about 330 Ma and 300 Ma, respectively. Thus, we consider it unlikely that either apparent grain-size, differences in mineral chemistry or a mixture of polytypes was responsible for controlling apparent diffusion-loss profiles in the muscovite analyzed. Instead, it is more likely that the presence of microstructures, intragranular recrystallization and chemical heterogeneity within the muscovite (*i.e*., subdomains) resulted in an effective grain-size with respect to argon diffusivity that is smaller than the finest size-fraction analyzed (<175 μm).

REFERENCES

ALEXANDER, E.C., MICHELSON, G.M. & LANPHERE, A. (1978): MMHb-1: a new ^{40}Ar/^{39}Ar dating standard. *In* Short Paper, 4th Int. Conf. on Geochronology, Cosmochronology and Isotope Geology. *U.S. Geol. Surv., Open-File Rep.* **78-701**, 6-8.

APPLEMAN, D.E. & EVANS, H.T., JR. (1973): Job 9214: indexing and least-squares refinement of powder diffraction data. *U.S. Geol. Surv., Comput. Contrib.* **20** (*NTIS Doc.* **PB2-16188**).

BALDWIN, S.L., HARRISON, T.M. & FITZ GERALD, J.D. (1990): Diffusion of ^{40}Ar in metamorphic hornblende. *Contrib. Mineral. Petrol.* **105**, 691-703.

BERGER, G.W. (1975): ^{40}Ar/^{39}Ar step heating of thermally overprinted biotite, hornblende and potassium feldspar from Eldora, Colorado. *Earth Planet. Sci. Lett.* **26**, 387-408.

_____ & YORK, D. (1981): Geothermometry from ^{40}Ar/^{39}Ar dating experiments. *Geochim. Cosmochim. Acta* **45**, 795-811.

CHATTERJEE, A.K. & CORMIER, R.F. (1991): A Rb–Sr geochronological study of the Davis Lake pluton, South Mountain Batholith, southern Nova Scotia: evidence for a 374 Ma time of emplacement. *In* Nova Scotia Dep. Mines & Energy Rep. Activities 1990 (D.R. MacDonald, ed.). *Nova Scotia Dep. Mines & Energy Rep.* **91-A**, 19.

_____ & HAM, L.J. (1991): U–Th–Pb systematics of the South Mountain Batholith, Nova Scotia. *Atlantic Geol.* **27**, 149 (abstr.).

CORMIER, R.F., KEPPIE, J.D. & ODOM, A.L. (1988): U–Pb and Rb–Sr geochronology of the Wedgeport granitoid pluton, southwestern Nova Scotia. *Can. J. Earth Sci.* **25**, 255-261.

COSTA, S. & MALUSKI, H. (1988): Use of the ^{40}Ar–^{39}Ar stepwise heating method for dating mylonite zones: an example from the St. Barthélémy Massif (northern Pyrénées, France). *Chem. Geol.* **72**, 127-144.

DALLMEYER, R.D. (1975): ^{40}Ar/^{39}Ar ages of biotite and hornblende from a progressively remetamorphosed basement terrane: their bearing on interpretation of release spectra. *Geochim. Cosmochim. Acta* **39**, 1655-1669.

_____ & KEPPIE, J.D. (1987): Polyphase late Paleozoic tectonothermal evolution of the southwestern Meguma Terrane, Nova Scotia; evidence from ^{40}Ar/^{39}Ar mineral ages. *Can. J. Earth Sci.* **24**, 1242-1254.

DALRYMPLE, G.B., ALEXANDER, E.C., JR., LANPHERE, M.A. & KRAKER, G.P. (1981): Irradiation of samples for ^{40}Ar/^{39}Ar dating using the Geological Survey TRIGA reactor. *U.S. Geol. Surv., Prof. Pap.* **1176**.

DODSON, M.H. (1973): Closure temperature in cooling geochronological and petrological systems. *Contrib. Mineral. Petrol.* **40**, 259-274.

FOLAND, K.A. (1974): ^{40}Ar diffusion in homogeneous orthoclase and an interpretation of Ar diffusion in K-feldspar. *Geochim. Cosmochim. Acta* **38**, 151-166.

GARVIE, R. (1986): LSUCRIPC, least-squares unit-cell refinement with indexing on the personal computer. *Powd. Diff.* **1**(1), 114.

GILETTI, B.J. (1991): Rb and Sr diffusion in alkali feldspar, with implications for cooling histories of rocks. *Geochim. Cosmochim. Acta* **55**, 1331-1343.

GOODWIN, L.B. & RENNE, P.R. (1991): Effects of progressive mylonitization on Ar retention in biotites from the Santa Rosa mylonite, California, and thermochronologic implications. *Contrib. Mineral. Petrol.* **108**, 283-297.

HAGGART, M.J., JAMIESON, R.A., REYNOLDS, P.H., KROGH, T.E., BEAUMONT, C. & CULSHAW, N.G. (1993): Last gasp of the Grenville Orogeny: thermochronology of the Grenville Front Tectonic Zone near Killarney, Ontario. *J. Geol.* **101**, 575-589.

HAM, L.J. & MACDONALD, M.A. (1991): Preliminary geological map of Wentworth Lake (NTS 21 A/O4). *Nova Scotia Dep. Natural Resources, Open File Map* **91-020** (scale 1:50 000).

HANSON, G.N., SIMMONS, K.R. & BENCE, A.E. (1975): ^{40}Ar/^{39}Ar spectrum ages for biotite, hornblende and muscovite in a contact metamorphic zone. *Geochim. Cosmochim. Acta* **39**, 1269-1277.

HARRISON, T.M. (1980): Diffusion of ^{40}Ar in hornblende. *Contrib. Mineral. Petrol.* **78**, 324-331.

_____, DUNCAN, I. & McDOUGALL, I. (1985): Diffusion of ^{40}Ar in biotite: temperature, pressure and compositional effects. *Geochim. Cosmochim. Acta* **49**, 2461-2468.

_____ & McDOUGALL, I. (1980): Investigations of an intrusive contact, northwest Nelson, New Zealand. I. Thermal, chronological and isotopic constraints. *Geochim. Cosmochim. Acta* **44**, 1985-2003.

_____, SPEAR, F.S. & HEIZLER, M.T. (1989): Geochronologic studies in central New England. II. Post-Acadian hinged and differential uplift. *Geology* **17**, 185-189.

HESS, J.C., LIPPOLT, H.J., GURBANOV, A.G. & MICHALSKI, I. (1993): The cooling history of the late Pliocene Eldzhurtinskiy granite (Caucasus, Russia) and the thermochronological potential of grain-size/age relationships. *Earth Planet. Sci. Lett.* **117**, 393-406.

HORNE, R.J., MACDONALD, M.A., COREY, M.C. & HAM, L.J. (1992): Structure and emplacement of the South Mountain Batholith, southwestern Nova Scotia. *Atlantic Geol.* **28**, 29-50.

KEPPIE, J.D. & DALLMEYER, R.D. (1987): Dating transcurrent terrane accretion: an example from the Meguma and Avalon composite terranes in the northern Appalachians. *Tectonics* **6**, 831-847.

———, KROGH, T.E. & DALLMEYER, R.D. (1993): Late Paleozoic P–T–t path for the Meguma Terrane, Nova Scotia: a history of collision, repeated crustal thickening, delamination, short-lived magmatism, rapid uplift and denudation. *Geol. Soc. Am., Abstr. Programs* **25**, A485.

KONTAK, D.J. (1990): The East Kemptville topaz–muscovite leucogranite, Nova Scotia. I. Geological setting and whole-rock geochemistry. *Can. Mineral.* **28**, 787-825.

——— (1991): The East Kemptville topaz–muscovite leucogranite, Nova Scotia. II. Mineral chemistry. *Can. Mineral.* **29**, 37-60.

——— (1994): Geological and geochemical studies of alteration processes in a fluorine-rich environment: the East Kemptville Sn-(Zn–Cu–Ag) deposit, Yarmouth County, Nova Scotia, Canada. *In* Alteration and Alteration Processes Associated with Ore-Forming Systems (D.R. Lentz, ed.). *Geol. Assoc. Can., Short Course Notes* **11**, 261-314.

——— & CHATTERJEE, A.K. (1992): The East Kemptville tin deposit, Yarmouth County, Nova Scotia: a Pb-isotope study of the leucogranite and mineralized greisens – evidence for a 366 Ma metallogenic event. *Can. J. Earth Sci.* **29**, 1180-1196.

——— & CORMIER, R.F. (1991): Geochronological evidence for multiple tectono-thermal overprinting events in the East Kemptville muscovite–topaz leucogranite, Yarmouth County, Nova Scotia, Canada. *Can. J. Earth Sci.* **28**, 209-224.

———, MULJA, T. & HINGSTON, R. (1986): The East Kemptville Sn deposit: preliminary results from recent mapping. *In* Tenth Annual Open House and Rev. of Activities (J.L. Bates & D.R. MacDonald, eds.). *Nova Scotia Dep. Mines & Energy, Information Ser.* **12**, 97-103.

MACDONALD, M.A., COREY, M.C., HAM, L.J. & HORNE, R.J. (1989): Petrographic and geochemical aspects of the South Mountain Batholith. *In* Mines & Minerals Branch, Rep. Activities 1989, Part A. (D.R. MacDonald & K.A. Mills, eds.). *Nova Scotia Dep. Mines & Energy, Rep.* **89-3**, 75-80.

———, HORNE, R.J., COREY, M.C. & HAM, L.J. (1992): An overview of recent bedrock mapping and follow-up petrological studies of the South Mountain Batholith, southwestern Nova Scotia, Canada. *Atlantic Geol.* **28**, 7-28.

MCDOUGALL, I. & HARRISON, T.M. (1988): *Geochronology and Thermochronology by the $^{40}Ar/^{39}Ar$ Method.* Oxford University Press, New York, N.Y.

MUECKE, G.K., ELIAS, P. & REYNOLDS, P.H. (1988): Hercynian/Alleghanian overprinting of an Acadian Terrane: $^{40}Ar/^{39}Ar$ studies in the Meguma Zone, Nova Scotia, Canada. *Chem. Geol.* **73**, 153-167.

PALMER, D.A.S. (1991): *Crystallochemical Characterization of White Micas from the East Kemptville Tin Deposit, Nova Scotia.* B.Sc. thesis, St. Francis Xavier Univ., Antigonish, Nova Scotia.

REYNOLDS, P.H., ELIAS, P., MUECKE, G.K. & GRIST, A.M. (1987): Thermal history of the southwestern Meguma Zone, Nova Scotia, from an $^{40}Ar/^{39}Ar$ and fission track dating study of intrusive rocks. *Can. J. Earth Sci.* **24**, 1952-1965.

——— & MUECKE, G.K. (1978): Age studies on slates: applicability of the $^{40}Ar/^{39}Ar$ stepwise outgassing method. *Earth Planet. Sci. Lett.* **40**, 111-118.

———, ZENTILLI, M. & MUECKE, G.K. (1981): K–Ar and $^{40}Ar/^{39}Ar$ geochronology of granitoid rocks from southern Nova Scotia: its bearing on the geological evolution of the Meguma Zone of the Appalachians. *Can. J. Earth Sci.* **18**, 386-394.

RICHARDSON, J.M. (1988): *Genesis of the East Kemptville Greisen-Hosted Tin Deposit, Davis Lake Complex, Southwestern Nova Scotia, Canada.* Ph.D. thesis, Carleton Univ., Ottawa, Ontario.

———, BELL, K., BLENKINSOP J. & WATKINSON, D.H. (1988): Fluid saturation textures and Rb–Sr isochron data from the East Kemptville tin deposit, southwestern Nova Scotia. *Geol. Surv. Can., Pap.* **88-1B**, 163-171.

———, SPOONER, E.T.C. & MCAUSLAN, D.A. (1982): The East Kemptville tin deposit, Nova Scotia: an example of a large tonnage, low grade, greisen-hosted deposit in the endocontact zone of a granite batholith. *Geol. Surv. Can., Pap.* **82-1B**, 27-32.

SCAILLET, S., FERAUD, G., BALLÈVRE, M. & AMOURIC, M. (1992): Mg/Fe and [Mg, Fe)Si–Al₂] compositional control on argon behaviour in high-pressure white micas: $^{40}Ar/^{39}Ar$ continuous laser-probe study from the Dora-Maira nappe of the internal western Alps, Italy. *Geochim. Cosmochim. Acta* **56**, 2851-2872.

SMITH, P.K. (1985): Mylonitization and fluidized brecciation in southern Nova Scotia. *In* Rep. Activities (K.A. Mills, ed.). *Nova Scotia Dep. Mines & Energy, Rep.* **85-1**, 119-133.

SNEE, L.W., SUTTER, J.F. & KELLY, W.C. (1988): Thermochronology of economic mineral deposits: dating the stages of mineralization at Panasqueira, Portugal, by high-precision $^{40}Ar/^{39}Ar$ age spectrum techniques on muscovite. *Econ. Geol.* **83**, 335-354.

STEIGER, R.H. & JÄGER, E. (1977): Subcommission on geochronology: Convention on the use of decay constants in geo- and cosmochronology. *Earth Planet. Sci. Lett.* **36**, 359-362.

TURNER, G. (1968): The distribution of potassium and argon in chondrites. *In* Origin and Distribution of the Elements (L.H. Ahrens, ed.). Pergamon Press, New York, N.Y. (387-398).

WEST, D.P., JR. & LUX, D.R. (1993): Dating mylonitic deformation by the $^{40}Ar – ^{39}Ar$ method: an example from the Norumbega Fault Zone, Maine. *Earth Planet. Sci. Lett.* **120**, 221-237.

WIJBRANS, J.R. & McDOUGALL, I. (1986): ^{40}Ar/^{39}Ar dating of white micas from an Alpine high-pressure metamorphic belt on Naxos (Greece): the resetting of the argon isotopic system. *Contrib. Mineral. Petrol.* **93**, 187-194.

_____ & _____ (1988): Metamorphic evolution of the Attic Cycladic metamorphic belt on Naxos (Cyclades, Greece) utilizing ^{40}Ar/^{39}Ar age spectrum measurements. *J. Metamorph. Geol.* **6**, 571-594.

WILLIAMS, H. & HATCHER, R.D., JR. (1983): Appalachian suspect terranes. *Geol. Soc. Am., Mem.* **158**, 33-53.

WRIGHT, T. & DALLMEYER, R.D. (1991): The age of cleavage development in the Ross orogen, northern Victoria Land, Antarctica: evidence from ^{40}Ar/^{39}Ar whole-rock slate ages. *J. Struct. Geol.* **13**, 677-690.

ZENTILLI, M. & REYNOLDS, P.H. (1985): ^{40}Ar/^{39}Ar dating of micas from the East Kemptville tin deposit, Yarmouth County, Nova Scotia. *Can. J. Earth Sci.* **22**, 1546-1548.

ZWENG, P.L., MORTENSEN, J.K. & DALRYMPLE, G.B. (1993): Thermochronology of the Camflo gold deposit, Malartic, Quebec: implications for magmatic underplating and the formation of gold-bearing quartz veins. *Econ. Geol.* **88**, 1700-1721.